Chemical Geology 362 (2013) 66–73

Contents lists available at ScienceDirect

Chemical Geology

journal homepage: www.elsevier.com/locate/chemgeo

Simulating Precambrian banded iron formation diagenesis

Nicole R. Posth [a,1], Inga Köhler [a], Elizabeth D. Swanner [a], Christian Schröder [b,c], Eva Wellmann [a], Bernd Binder [a], Kurt O. Konhauser [d], Udo Neumann [e], Christoph Berthold [e], Marcus Nowak [e], Andreas Kappler [a,*]

[a] Geomicrobiology, Center for Applied Geoscience, University of Tuebingen, Sigwartstrasse 10, 72076 Tuebingen, Germany
[b] Environmental Mineralogy, Center for Applied Geoscience, University of Tuebingen, Sigwartstrasse 10, 72076 Tuebingen, Germany
[c] Department of Hydrology, University of Bayreuth, Germany
[d] Department of Earth and Atmospheric Sciences, University of Alberta, Edmonton, Alberta, T6G 2E3, Canada
[e] Mineralogy & Geodynamics, Department of Geosciences, University of Tuebingen, Wilhelmstrasse 56, 72074 Tuebingen, Germany

ARTICLE INFO

Article history:
Accepted 27 May 2013
Available online 6 June 2013

Keywords:
Mineral diagenesis
Mineral transformations
Banded iron formations
Anoxygenic phototrophs
Biogenic minerals

ABSTRACT

Post-depositional diagenetic alteration makes the accurate interpretation of key precipitation processes in ancient sediments, such as Precambrian banded iron formations (BIFs), difficult. While microorganisms are proposed as key contributors to BIF deposition, the diagenetic transformation of precursor Fe(III) minerals associated with microbial biomass had not been experimentally tested. We incubated mixtures of ferrihydrite (proxy for biogenic ferric oxyhydroxide minerals) and glucose (proxy for microbial biomass) in gold capsules at 1.2 kbar and 170 °C. Both wet chemical analysis and mineralogical methods (microscopy, X-ray diffraction and Mössbauer spectroscopy) were used to analyze the reaction products. Under these conditions, ferrihydrite ($Fe^{III}(OH)_3$) transforms to hematite ($Fe^{III}_2O_3$), magnetite ($Fe^{II}Fe^{III}_2O_4$), and siderite ($Fe^{II}CO_3$). Silica-coated ferrihydrite prepared at conservative Si:Fe ratios (as predicted for the Precambrian oceans) and mixed with glucose yielded hematite and siderite, whereas magnetite could not be identified microscopically. Our results show that electron transfer from organic carbon to Fe(III) minerals during temperature/pressure diagenesis can drive the production of key BIF minerals. Our results also demonstrate that the post-depositional mineralogy of BIF does not directly archive the oceanic or atmospheric conditions present on Earth during their lithification. As a consequence, atmospheric composition regarding concentrations of methane and CO_2 during the time of BIF mineral deposition cannot be directly inferred from BIF mineralogical data alone.

1. Introduction

Low-grade diagenetic to metamorphic overprinting by temperature and pressure yields secondary minerals that obscure our understanding of primary depositional mechanisms (Han, 1966; Dimroth and Chauvel, 1973; Perry et al., 1973; Han, 1978; Walker, 1984; Klein, 2005; Bekker et al., 2010). This poses a barrier to the reconstruction of early Earth environments using ancient sediments, such as banded iron formations (BIFs). The principal era of deposition of these complex rocks occurred between 3.8 and 1.8 billion years ago, a timeframe which spans the transition from an anoxic to an oxic world (e.g. Anbar et al., 2007). As both marine geochemical and microbial processes are thought to have driven BIF deposition, these sediments offer an archive of the hydrosphere, atmosphere and biosphere at the time when they formed. However, in order to use BIFs as an archive of the past, the diagenetic transformation of sediments that compose BIF during and after burial must be assessed (Konhauser et al., 2005; Posth et al., 2008).

At the time of BIF deposition, the oceans were anoxic and rich in both dissolved Fe(II) (0.05–0.5 mM; Holland, 1973; Morris, 1993) and silica (2.20 mM; Maliva et al., 2005). Dissolved Fe(II) is believed to have been largely sourced from hydrothermal vents (Holland, 1973), while silica came largely from the continents (Hamade et al., 2003). The primary minerals were most likely (ferro-) ferric oxyhydroxides, such as ferrihydrite ($Fe(OH)_3$), greenalite ($(Fe)_3Si_2O_5(OH)_4$), siderite ($FeCO_3$), and amorphous silica ($SiO_2 \cdot nH_2O$). By contrast, the mineral assemblages found today in the lowest grade metamorphosed BIF include chert (SiO_2), magnetite (Fe_3O_4), hematite (Fe_2O_3), iron carbonates such as siderite and ankerite ($Ca(Fe,Mg,Mn)(CO_3)_2$), and various iron-silicate phases (Dimroth and Chauvel, 1973; Walker, 1984; Neumann and Mücke, 1994; Klein, 2005).

Today it is believed that the deposition of BIF is intimately linked to microbial activity (e.g., Konhauser et al., 2007a; , 2007b; Planavsky et al.,

* Corresponding author at: Geomicrobiology, Center for Applied Geoscience, University of Tuebingen, Sigwartstr. 10, 72076 Tuebingen, Germany. Tel.: +49 7071 29 74992; fax: +49 7071 29 5059.
E-mail address: andreas.kappler@uni-tuebingen.de (A. Kappler).
[1] Present address: Nordic Center for Earth Evolution (NordCEE), Institute for Biology, University of Southern Denmark, Campusvej 55, 5230 Odense M, Denmark.

0009-2541/$ – see front matter © 2013 Elsevier B.V. All rights reserved.
http://dx.doi.org/10.1016/j.chemgeo.2013.05.031

2009; Posth et al., in press). The earliest biological models invoked the reaction between dissolved Fe(II) and cyanobacterially-produced O_2, most likely in localized oxic surface marine waters, i.e., in association with planktonic blooms (e.g., Cloud, 1968). Other bacteria may have played a more direct role in Fe(II) oxidation. For example, Holm (1989) speculated that oxidation of Fe(II) by chemolithoautotrophic species such as *Gallionella ferruginea* would have been kinetically favored in an ocean with limited free oxygen. Indeed, many of the 1.9 Gyr old Gunflint-type microfossils can be interpreted as chemolithoautotrophic Fe(II)-oxidizers (Planavsky et al., 2009). These O_2-based BIF models, however, must by necessity post-date the origins of cyanobacteria, currently believed to have evolved around 2.8–2.7 Ga (e.g., Summons et al., 1999). Under anoxic conditions, a different biological mechanism has been proposed for BIF deposition; the direct oxidation of Fe(II) by anoxygenic phototrophs (photoferrotrophy) (Widdel et al., 1993; Konhauser et al., 2002; Kappler et al., 2005; Posth et al., 2008, 2011, in press).

Any microbial activity in a BIF basin would have resulted in the deposition of microbial biomass. In sediment, mainly biotic processes degrade organic matter and lead to secondary mineral phases. Photoferrotrophy produces biogenic Fe minerals that differ from their abiogenic counterparts as they consist of a mixture of Fe(III) minerals and bacterial organic matter (Posth et al., 2010). In the Archean, Fe(III) and biomass (CH_2O) would have driven bacterial fermentation and respiration of organic carbon by Fe(III) reduction and methanogenesis. Microbial Fe(III) reduction yields Fe^{2+} which can react with Fe(III) minerals to form magnetite or precipitate as Fe(II) minerals, such as siderite or the mixed valence green rust ($[Fe^{II}_{(6-x)}Fe^{III}_{x}(OH)_{12}]^{x+}[(A^{2-})_{x/2} \cdot yH_2O]^{x-}$) (Thamdrup, 2000; Hansel et al., 2003). The average oxidation state of BIF, $Fe^{2.4+}$ (Klein, 2005), suggests either the simultaneous deposition of Fe(II) and Fe(III) or the post-depositional diagenetic alteration of ferric iron precipitates (Konhauser et al., 2005). Textural evidence from BIF indicates that the mixed valence Fe minerals were more likely caused by post-depositional reactions of Fe(III) minerals (Krapež et al., 2003). Indeed, stable isotope (Fe, C, O) and ecophysiological studies support the involvement of Fe(III)-reducing microorganisms in siderite and magnetite formation in short term BIF diagenesis (Johnson et al., 2008; Heimann et al., 2010; Craddock and Dauphas, 2011).

Yet, some cell organic carbon associated with iron minerals is not consumed by biotic or abiotic processes and may be recalcitrant over longer time frames than first believed. A recent study estimates that 23–27% of total organic carbon remains bound to reactive iron oxides in mature (100,000 year old) Fe-rich marine sediments (Lalonde et al., 2012). The fate of such aggregates consisting of Fe(III) minerals and organic carbon over deep time and the expected transformations at elevated temperature and pressure can be estimated thermodynamically. However, they have not been thoroughly demonstrated experimentally. Indeed, there is still much to learn about the mechanism of organic carbon preservation by iron as well as the diagenesis and long-term burial of Fe(III)-organic carbon complexes (Eglinton, 2012).

Three questions motivate our study: (1) do reactions proceed according to thermodynamic estimates, (2) does the transformation of ferrihydrite in the presence or absence of CH_2O yield the same products and (3) do the transformations of biogenic Fe(III) minerals harbor unique structural biosignatures such as specific structural arrangement, intergrowth, and/or rim formation? To address these questions, we incubated a mixture of chemically-synthesized ferrihydrite and glucose in gold capsules at 170 °C and 1.2 kbar pressure. This mixture of ferrihydrite and glucose functioned as a proxy of biogenic Fe(III) minerals. Two different proportions of the ferrihydrite and glucose were tested and based on previous study of biogenic Fe(III) minerals produced by anoxygenic phototrophic bacteria (Posth et al., 2010). The incubation conditions chosen were based on those estimated for South African Transvaal Supergroup BIF (Miyano and Klein, 1984; Miyano, 1987). The resulting iron redox state, mineral product identity and mineral assemblages were documented.

2. Methods and sample preparation

2.1. Chemically-synthesized reagents

We synthesized ferrihydrite (Fig. 1(1)) according to the standard method developed by Cornell and Schwertmann (2003). Synthesized ferrihydrite alone was used in our experiments to create a proxy of abiogenic Fe(III) oxyhydroxide minerals. Abiogenic minerals are produced in the environment by the chemical oxidation of Fe(II) by O_2 and are not deposited together with cells. We then used a mixture of the synthesized, abiogenic ferrihydrite and glucose as a proxy of biogenic Fe(III) minerals. In the environment, biogenic minerals are produced, for example, by anoxygenic Fe(II)-oxidizing phototrophic bacteria (Cornell and Schwertmann, 2003; Kappler and Newman, 2004). These biogenic minerals are cell-mineral aggregates and can be described as networks of cells, i.e. organic matter, and Fe(III) oxyhydroxide minerals (Posth et al., 2010). Silica-coated ferrihydrite was synthesized using the same method in the presence of 2.2 mM dissolved silica. Both minerals, i.e. the synthesized ferrihydrite and the Si-coated ferrihydrite, were freeze-dried and subsequently identified as 2-line ferrihydrite via μ-X-ray diffraction (μ-XRD) and Mössbauer spectroscopy (Sharma et al., 2010). They were then stored in the dark at 4 °C and used within a 2 month period. Glucose (α-D(+)-Glucose monohydrate, $C_6H_{12}O_6 \cdot H_2O$ (>99.5%, Carl Roth, Germany)) was used as a biomass proxy. Ferrihydrite and glucose were chosen instead of hematite and more recalcitrant organic matter as it was necessary for the experimental compounds to (1) have a high reactivity (experimental run time is one in which mineral transformations can be realistically traced), (2) be produced in a reproducible quality and composition, and (3) be relevant as a proxy for both the mineral deposition process and microbial cells in appropriate element ratios.

2.2. Gold capsule preparation

Gold capsules were prepared out of meter-long gold tubing (2.5 mm outer diameter, 0.2 mm wall thickness) and cut into approximately 2.7–3.0 cm long pieces (1.13–1.25 cm^3 inner volume). The capsules were baked at 800 °C for 4 h to remove oils and processing remnants. One side was crimped and welded shut before the empty capsule was weighed (Fig. 1(2)). The glucose and ferrihydrite mixtures were mixed thoroughly with a mortar and pestle, checked microscopically for consistent blending and filled into the capsules with a funnel (SI.A).

In order to minimize air between the grains air, the minerals were compacted into the capsule with a 2 mm diameter metal mallet until full (SI.B). Theoretically, however, the available capsule volume filled with mineral and compacted to capacity in the open air would result in the oxidation of less than 1% of the glucose in the capsule during diagenesis experiments (for calculation, SI.B).

After filling, the capsules were crimped shut with pliers and sealed on both sides with an arc welding process employing a graphite electrode (Fig. 1(3)). During welding, the capsules were cooled with ice water in order to prevent thermal reactions prior to the P/T treatment. The full capsules were weighed once more and placed in an ultrasonic bath for approximately 15 min, dried at 60 °C, and weighed once again. Incomplete welding of the capsule was detectable by an increase in mass due to the entry of water to the capsule during ultrasonication. Two gold capsules for each experiment were placed in externally heated rapid heat, rapid quench autoclaves or cold-seal pressure vessels for different time spans of 1, 7, 10, 14, 28, 40 and 137 days at 170 °C and 1.2 kbar (Fig. 1(4)). At the end of the temperature and pressure treatment, capsules were dried at 60 °C

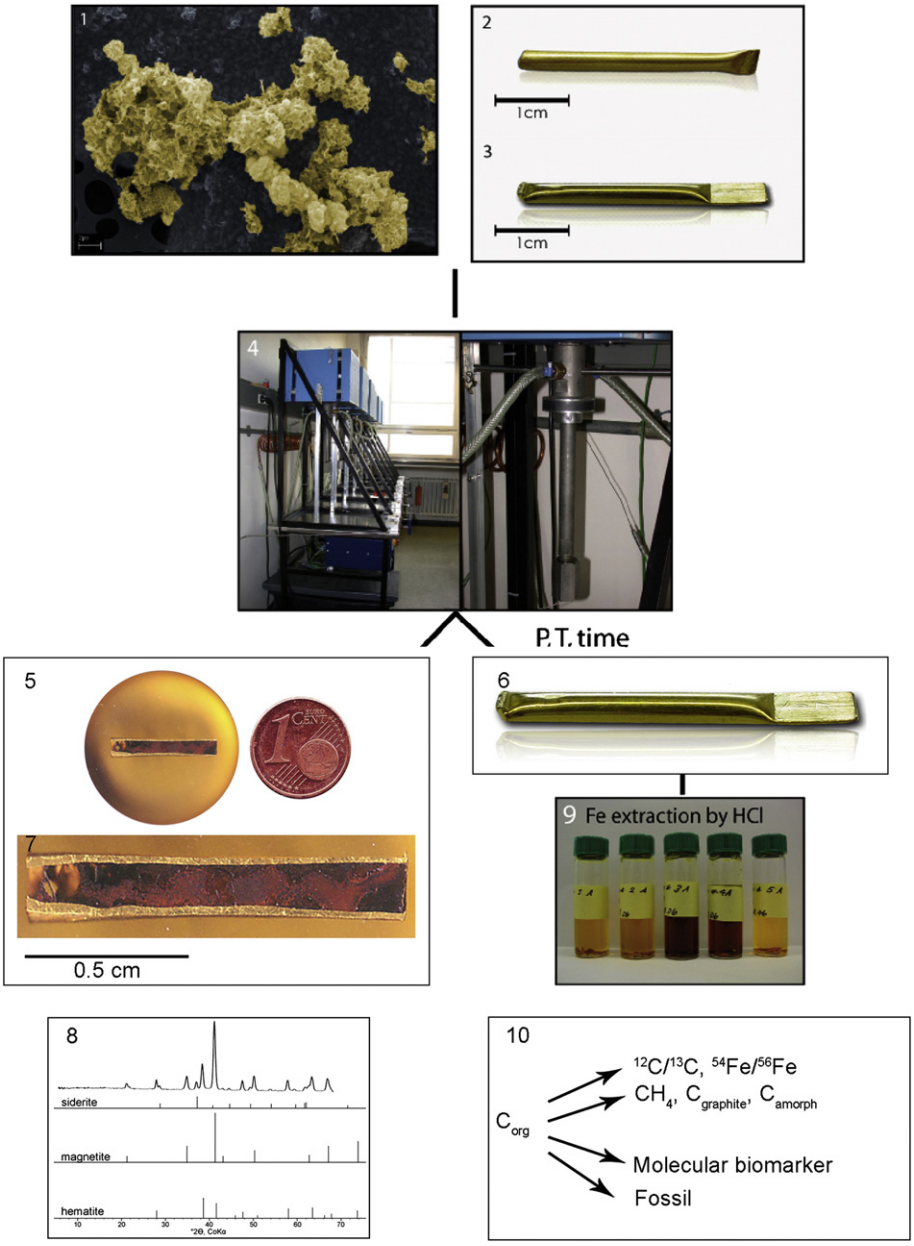

Fig. 1. Scheme of the experimental approach. Chemically synthesized ferrihydrite (1) or a mixture of ferrihydrite and glucose are tightly packed into gold capsules (2), sealed (3), and placed in high temperature and pressure autoclaves (4). After P/T-treatment, samples are analyzed via mineralogical methods (microscopy, XRD, Mössbauer spectroscopy) and by wet-chemical methods (sequential extraction) (5–9) and will be analyzed in the future also for isotope composition, carbonaceous compounds and molecular and structural biomarkers (10).

and weighed. Analysis of capsules incubated for different lengths of time showed that the main mineral transformations occurred within the first 14 days. Herein, we therefore focus on data from 14-day capsules. A detailed study describing the temporal development of mineral crystallinity, crystal size, and mineral phase proportions will be presented in a separate report.

The transformation of glucose or ferrihydrite during capsule preparation (including the welding process) was investigated in a control experiment. One capsule was filled with ferrihydrite and glucose, closed as described above, and left at standard temperature and pressure (STP). The capsule was then embedded in epoxy resin and ground open. The resulting ferrihydrite-glucose mixture consisted of small, white grains which were black to brown in color (not shown). These were interpreted as glucose and demonstrated no transformation of the ferrihydrite and glucose during capsule preparation.

2.2.1. Rationale for ratios of ferrihydrite and glucose

The first set of capsules was filled with 100 mg of chemically-synthesized ferrihydrite and 4.23 mg glucose. Theoretically, complete oxidation of carbon in glucose to CO_2 and reduction of Fe(III) to Fe(II) in the capsules results in a 0.6 ratio of the electrons released by carbon to the electrons consumed by Fe(III). This “0.6 ratio” of ferrihydrite to glucose was chosen to mimic a scenario in which an excess of Fe(III) to biomass prevails in the sediment and is herein referred to as such.

In the anoxygenic Fe(II)-oxidizing phototroph model of BIF deposition in the Archean ocean, biogenic mineral precipitation would likely have been characterized by the complete sedimentation of heavy iron hydroxides and deposition of a fraction of the biomass produced (50–96%, depending on the concentration of Fe(II) in solution (Konhauser et al., 2005; Posth et al., 2010)). Partial deposition of the biomass is reasonable considering its lower density and lower sedimentation

rates (Posth et al., 2010). This would lead at least to partial degradation of the biomass in the water column, for example, by fermentation and methanogenesis. However, there are also scenarios in which excess biomass would be deposited in relation to biogenic ferric oxides, such as hydrothermal systems like a plume in which other electron donors are also present (HS^-, H_2 or organic compounds in addition to Fe^{2+}). To mimic these scenarios in which an excess of biomass to Fe(III) mineral prevails, experiments were also performed with a 2.4 electron ratio. These experiments are referred to herein as "2.4 ratio".

A third set of experiments were designed to test the influence of silica on the ferrihydrite–glucose system. Ferrihydrite was chemically-synthesized according to Cornell and Schwertmann (2003) in the presence of 2.2 mM dissolved silica. This concentration of dissolved silica resulted in a conservative Si:Fe ratio of 0.075 (2.26 mg Si to 111 mg Fe), a value much lower than the highest estimates for the Archean.

2.3. Autoclaves

The autoclaves (Fig. 1(4)) at the Institute for Geosciences at the University of Tuebingen consist of a nickel-chromium alloy (Inconel 713 LC). They are designed to apply pressures of 1 bar to 5 kbar and temperatures of 20 °C to 800 °C onto a small volume of space inside a sample chamber. For this study, a maximum of two capsules were placed into one water-filled chamber. The autoclaves were set to reach 170 °C and 1.2 kbar. After adjusting pressure (P) and temperature (T), the capsules were transferred from a water cooled section of the autoclave into a hot zone using a movable magnet. Likewise, at the end of the experimental phase, the capsules were cooled with a rapid quench technique to stop further mineral transformation or crystallization processes that would occur during slow cooling. To this end, the capsules were dropped from the sample chamber into a water cooled section of the autoclave (Fig. 1(4)). Using these autoclaves, capsules were incubated to prepare thick sections for microscopy.

Additionally, cold-seal pressure vessels were used to incubate capsules for bulk XRD and Mössbauer spectroscopy analysis. These autoclaves consist of a vessel built from a Rene 41 alloy rod. A hole is drilled into the rod to hold 2 gold capsules. The cold-seal pressure vessels are designed to apply temperatures of up to 800 °C and pressures of up to 5 kbar. For these experiments, the autoclaves were set to a target temperature of 170 °C and a pressure of 1.2 kbar. To terminate the incubation period in the autoclave, the vessel was cooled by compressed air within minutes.

2.4. Analytical methods

For each experimental set-up, 0.6 ratio ferrihydrite–glucose, 2.4 ratio ferrihydrite–glucose and silica-coated ferrihydrite–glucose, parallel capsules were prepared. One capsule was embedded in casting resin (Körapox 439®, Kömmerling) for mineral characterization (Fig. 1(5)). The other was used for laboratory-based analysis, such as iron redox species quantification (Fig. 1(6, 9)). Mineral and mineral inclusion identification was carried out by reflected light microscopy, μ-X-ray diffraction (XRD) (Fig. 1(7, 8)), Mössbauer spectroscopy, and μ-Raman spectroscopy as described in SI. C in Appendix A. Both Fe(II) and Fe(III) were quantified by chemical extraction and subsequent spectrophotometric analysis, as well as by Mössbauer spectroscopy. For details see SI.C.

3. Results and discussion

3.1. Ferrihydrite–glucose diagenesis by P/T — iron redox speciation analysis

After an incubation time of 14 days in the autoclave, HCl extraction of capsules filled with ferrihydrite alone yielded 100% Fe(III) (not shown). In contrast, the Fe(II)/Fe(tot) ratio in ferrihydrite–glucose capsules with a 0.6 electron ratio was 0.13 ± 0.05. Mössbauer spectroscopy analysis of two independent ferrihydrite–glucose capsules also yielded Fe(II)/total Fe ratios of 0.14 ± 0.04 and 0.23 ± 0.04 (SI.D) and suggest rapid reduction of Fe(III) to Fe(II) by transfer of electrons from the glucose to Fe(III). The remaining reducing equivalents from glucose after treatment could be present in the form of reduced gases (H_2 or CH_4) or elemental carbon. We propose that in the case of elemental carbon formation, the reducing equivalents in the carbon are physically separated from the Fe(III) via an Fe(II)-containing mineral barrier and therefore not easily available for further reduction of Fe(III) to Fe(II) within the timeframe of our experiment.

3.2. Ferrihydrite–glucose diagenesis — P/T-mineral analyses

Mixtures of glucose and chemically-synthesized ferrihydrite treated at 170 °C and 1.2 kbar developed a crystalline, whitish mineral phase (Fig. 2 and SI. C in Appendix A) that also formed when ferrihydrite was incubated without glucose (not shown). Red internal reflections and minor bireflectance identify this mineral as hematite (Fig. 2A,B), in accordance with the established dehydration reaction of ferrihydrite to hematite under the influence of heat (reaction (1); Cornell and Schwertmann, 2003):

$$2Fe(OH)_3 \rightarrow Fe_2O_3 + 3H_2O. \quad (1)$$

Theoretically, a mixture of ferrihydrite and glucose consistent with natural sediment where Fe(III) minerals and organic carbon are present, yields siderite ($FeCO_3$), magnetite (Fe_3O_4) and elemental carbon under temperature and pressure. Water, methane (CH_4) and hydrogen gas (H_2) could be released by dehydration and coupled redox reactions, including biomass oxidation and Fe(III) reduction (represented by CH_2O; reaction (2)):

$$Fe(OH)_3 \text{ or } Fe_2O_3 + CH_2O \rightarrow Fe^{III}_2O_3, Fe^{II}CO_3, Fe^{II}Fe^{III}_2O_4, CH_4, C, H_2, H_2O. \quad (2)$$

Indeed, incubated ferrihydrite and glucose yielded ~20 μm crystals that often formed large aggregates (Fig. 2B). Strong bireflectance, strong anisotropism and light internal reflection under crossed polars were indicative of siderite. It is plausible that this siderite formed from ferrihydrite and CH_2O (reaction (3)). As H_2 has not yet been quantified, it is unclear whether siderite formed together with H_2 (reaction (4)):

$$4Fe(OH)_3 + CH_2O \rightarrow FeCO_3 + 3Fe^{2+} + 6OH^- + 4H_2O \quad (3)$$

$$2Fe(OH)_3 + 2CH_2O \rightarrow 2FeCO_3 + 2H_2O + 3H_2. \quad (4)$$

Siderite was also found in association with hematite crystals (Fig. 2B) suggesting another formation pathway from hematite and biomass (reaction (5) or (6)):

$$2Fe_2O_3 + CH_2O + 2H_2O \rightarrow FeCO_3 + 3Fe^{2+} + 6OH^- \quad (5)$$

$$Fe_2O_3 + 2CH_2O + H_2O \rightarrow 2FeCO_3 + 3H_2. \quad (6)$$

Aside from siderite, magnetite was identified by its fine gray to white color and its net-like primary particles (2–4 μm that lacked both internal reflections and anisotropism; Fig. 2B). A number of magnetite formation pathways are theoretically possible under our experimental conditions. Three main pathways to magnetite are described (Frost et al., 2007; Pecoits et al., 2009; Li et al., 2013). First, ferrihydrite, or hematite formed from ferrihydrite could be partially re-reduced by organic carbon (reaction (7) or (8)):

$$12Fe(OH)_3 + CH_2O \rightarrow 4Fe_3O_4 + CO_2 + 19H_2O \quad (7)$$

$$6Fe_2O_3 + CH_2O \rightarrow 4Fe_3O_4 + CO_2 + H_2O. \quad (8)$$

Second, magnetite production could be driven by the partial oxidation of Fe(II) or Fe(II) minerals by CO_2. Siderite oxidation could produce magnetite along with methane (reaction (9)) and has been reported for 450 °C and 2 kbar (French, 1971; McCollom, 2003; Marocchi et al., 2011).

$$12FeCO_3 + 2H_2O \rightarrow 4Fe_3O_4 + 11CO_2 + CH_4 \quad (9)$$

Third, the juxtaposition of hematite and ferrous iron like siderite would favor magnetite production (reaction (10)) (Burt, 1972). This was estimated to occur at 220–280 °C and 1–2 kbar (Miyano, 1987) and has been shown experimentally at ~370 °C and 2 kbar (French, 1971) (reaction (10)).

$$FeCO_3 + Fe_2O_3 \rightarrow Fe_3O_4 + CO_2 \quad (10)$$

Yet, a fourth magnetite forming reaction is also possible between Fe(III) minerals and Fe^{2+} for example in hydrothermal settings, such as the Algoma-type banded iron formations (Ohmoto, 2003)(reaction (11) or (12)):

$$2Fe(OH)_3 + Fe^{2+} \rightarrow Fe_3O_4 + 2H_2O + 2H^+ \quad (11)$$

$$Fe_2O_3 + Fe^{2+} + H_2O \rightarrow Fe_3O_4 + 2H^+. \quad (12)$$

Textural evidence for magnetite formation through a reaction of $Fe(OH)_3$ and Fe^{2+} has also been presented for some of the Lake Superior and Pilbara BIF (Han, 1978).

In the present study, magnetite was often found close to siderite within a poorly crystalline hematite matrix and along the rims of sharply-defined hematite (Fig. 2B), suggesting it formed from organic carbon and ferrihydrite or hematite (reactions (7) and (8)). This association of magnetite and hematite has been discussed in relation to several iron formations (Robbins and Iberall, 1991). Magnetite crystals within siderite and along siderite rims (Fig. 2B) also suggest their formation via siderite oxidation (reaction (9)). Based on the spatial association between the magnetite and siderite, however, the formation of these minerals more likely results from a reaction of hematite with organic carbon yielding magnetite, siderite and either hydrogen or Fe^{2+} (reaction (13) or (14)):

$$2Fe_2O_3 + CH_2O \rightarrow Fe_3O_4 + FeCO_3 + H_2 \quad (13)$$

$$10Fe_2O_3 + 3CH_2O + 10H^+ \rightarrow 4Fe_3O_4 + 3FeCO_3 + 5Fe^{2+} + 8H_2O. \quad (14)$$

Bulk XRD analysis of the capsule content (Fig. 2C) confirmed the presence of siderite, magnetite and hematite. Mössbauer spectroscopy subsequently quantified the relative amounts of these minerals, measured both at 140 K and room temperature (RT) (SI.B). The most abundant phases were hematite (49 ± 4 wt.% (140 K); 60 ± 4 wt.% (RT)), followed by magnetite (33 ± 4 wt.% (140 K); 33 ± 4 wt.% (RT)), and siderite (19 ± 6 wt.% (140 K); 7 ± 6 wt.% (RT)). Ferrihydrite was not detected after 14 days.

Interestingly, aside from hematite, siderite and magnetite, a light gray, monocline mineral several 100 μm in size was identified with Raman spectroscopy as humboldtine (SI.E). Although humboldtine, an iron oxalate with the formula $Fe^{II}(C_2O_4) * 2H_2O$, is not present in BIF today and not expected to survive higher temperatures (~355 °C; Frost and Weier, 2004), it is a possible intermediate phase.

To determine the effect of different amounts of biomass deposited together with ferric oxyhydroxides on the identity and quantity of minerals formed during diagenesis, samples with an organic carbon to ferrihydrite electron ratio of 0.6 and 2.4 were compared (Fig. 3). Samples with an electron ratio of 2.4 represent a scenario with a surplus of microbial biomass compared to Fe(III), like a vent system with additional electron donors (HS^-, H_2) present for CO_2 fixation and biomass formation. After 14 days, samples with excess carbon (ratio 2.4) formed siderite and magnetite (Fig. 3A). The siderite had

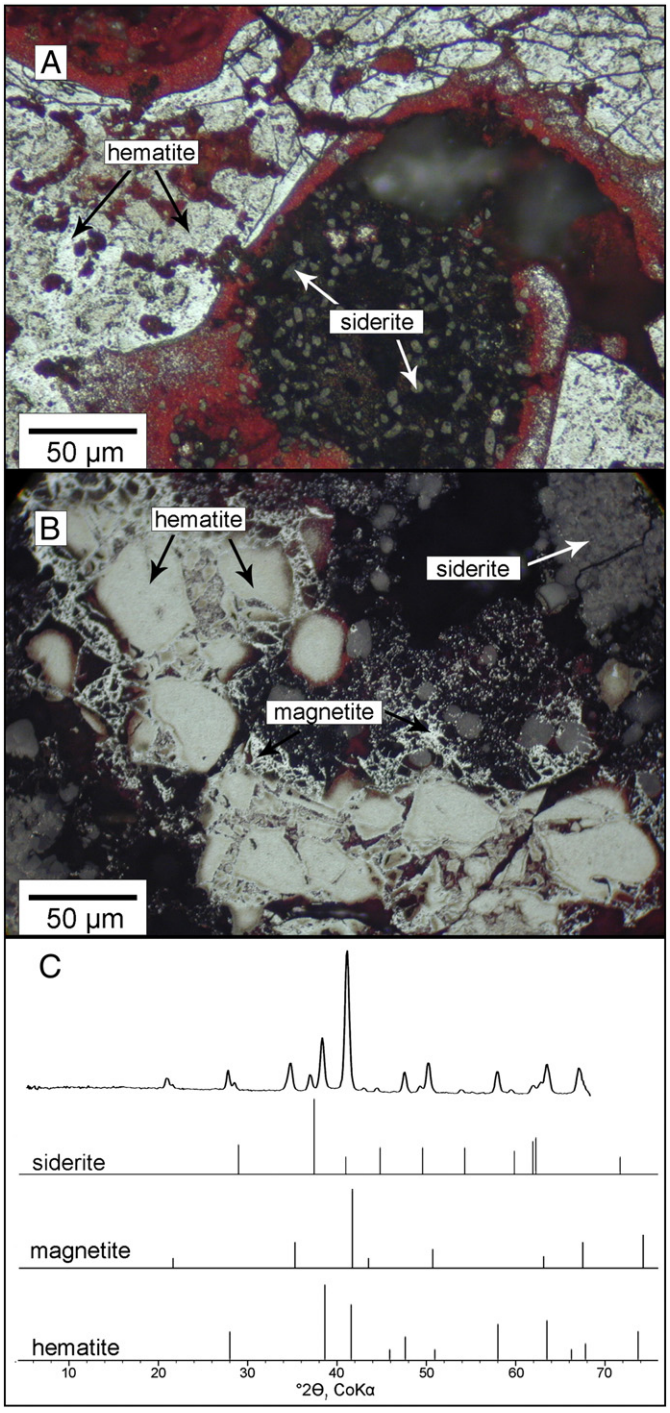

Fig. 2. Reflected light microscopy images (A, B) with surplus Fe (electron ratio 0.6) after 14 days incubation time. Globular to rhombic siderite crystals and black, poorly crystalline hematite are visible (SI. E in Appendix A, Fig. E-1). Magnetite seen as net-like structures and finely grained within siderite crystals and Fe(III) oxide matrix. (C) Hematite, magnetite and siderite identified by bulk XRD (powder, 300 μm spot size). Reference lines for hematite, magnetite, and siderite (ICDD PDF-2 database numbers 033-0664, 019-0629, and 029-0696).

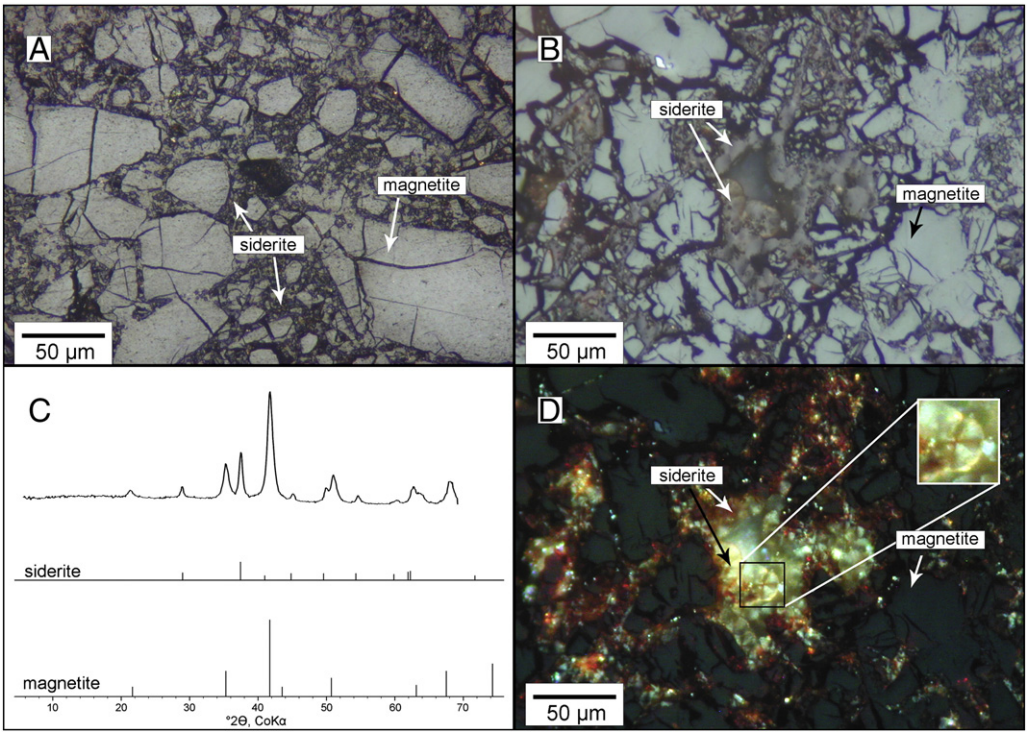

Fig. 3. Reflected light microscopy of mineral transformation with surplus glucose (electron ratio 2.4) (A, B) indicates siderite and magnetite. Bulk XRD (powder, spot size of 300 μm) (C) shows magnetite and siderite. (D) Siderite strongly anisotropic under crossed polars. The insert shows globular siderite with indicative cross structures.

globular structures similar but smaller than those in electron ratio 0.6 set-ups (Fig. 3A,B). Ferrihydrite and hematite were not detected by light microscopy. X-ray diffraction of the bulk material identified siderite and magnetite, but no hematite (Fig. 3C). Furthermore, the siderite in the 2.4 ratio capsules showed uniaxial extinction under crossed polars (Fig. 3D) which was not seen in 0.6 ratio samples. Such sideritic spherulites, common to many iron formations, are typical diagenetic features (Koehler et al., 2013). Due to their apatite cores, a biogenic origin has been proposed for these features in BIF (Heaney and Veblen, 1991). Our observation that increasing amounts of biomass in capsules containing ferrihydrite leads to formation of these characteristic siderite structures correlates well with a biogenic hypothesis.

A surplus of organic carbon should provide enough electrons to a complete reduction of the Fe(III) in magnetite to form siderite. In order to test whether the complete reduction to siderite would take place with time, 7, 14, 28 and 40 day incubations with an excess of biomass were performed. Magnetite was detected microscopically and with Mössbauer at every time point (data not shown). The higher carbon content seemingly favored the fast formation of magnetite and suggests a similar effect in BIF deposition in basins with high biomass sedimentation. Indeed, Walker (1984) linked the progressive reduction of Fe(III) during diagenesis to increasing amounts of reduced carbon in the system. The increasing amount of carbon would drive the replacement of hematite (or ferrihydrite) by magnetite, which in turn, could be replaced by siderite via further reduction of the magnetite. Yet, the relative proportions of magnetite and siderite changed over time (data not shown) and magnetite formed despite an excess of organic carbon reducing equivalents. If the reaction indeed proceeds to siderite over months or years, then the presence of magnetite in BIF could indicate a specific restricted concentration of biomass.

3.3. The influence of silica on the diagenesis of ferrihydrite–glucose mixtures

The presence of silica was expected to alter the transformation of Fe(III) minerals, for example, as changing surface charge inhibits mineral nucleation (Schwertmann, 1966; Jones et al., 2009). The Fe(II)/Fe_{tot} ratio (0.20 ± 0.02) of silica-coated ferrihydrite/glucose incubations at 0.6 electron ratio was comparable to that of experiments without silica (HCl extractions (0.13 ± 0.05); Mössbauer spectroscopy (0.14 ± 0.04 and 0.23 ± 0.04)). After incubation, reflected light showed a fined-grained hematite matrix surrounding siderite (SI.F). In parallel incubations, particles of the rare mineral humboldtine with its typical elongated tabular morphology were also visible both under reflected light and internal light reflection under crossed polars (Koehler et al., 2013). Magnetite and silicate phases were not identified microscopically in all cases. The Si:Fe ratio of these experiments was conservative (0.075), being much lower than the highest estimates for the Archean ocean (~4.4; Maliva et al., 2005; Konhauser et al., 2007a). Nonetheless, the lack of a magnetite product shows that ferrihydrite reactivity changed. The presence of silica in these incubations, however, did not fully hinder a reaction between ferrihydrite and glucose as siderite and humboldtine still form and Fe(II)/Fe(III) ratios and Fe mineralogy were comparable to the silica-free experiments.

3.4. Implications and limitations of ferrihydrite–glucose diagenesis studies

Chemically-synthesized ferrihydrite alone transforms to hematite via dehydration at elevated temperature and pressure, while capsules containing ferrihydrite and a biomass proxy (glucose) yield hematite, magnetite and siderite (Fig. 4A). As not just hematite, but siderite and magnetite are found in BIF, the results of this study confirms that biomass in BIF depositional basin sediment was important for the transformation of precursor sediments to the minerals present today (Walker, 1984; Konhauser et al., 2005; Johnson et al., 2008; Li et al., 2011). Furthermore, the ratio of cell biomass proxy to Fe(III) mineral effected the minerals formed (Fig. 4B). Yet, caution must be taken in interpreting siderite and magnetite in BIF as a marker for the primary presence of biomass. For example, in Fe-rich-systems, high amounts of dissolved CO_2 could drive the abiotic precipitation of siderite (Konhauser et al., 2007a). Similarly, reactions between Fe(III) minerals and Fe^{2+} in hydrothermal areas (reactions (11)–(12)) can form magnetite (Ohmoto, 2003).

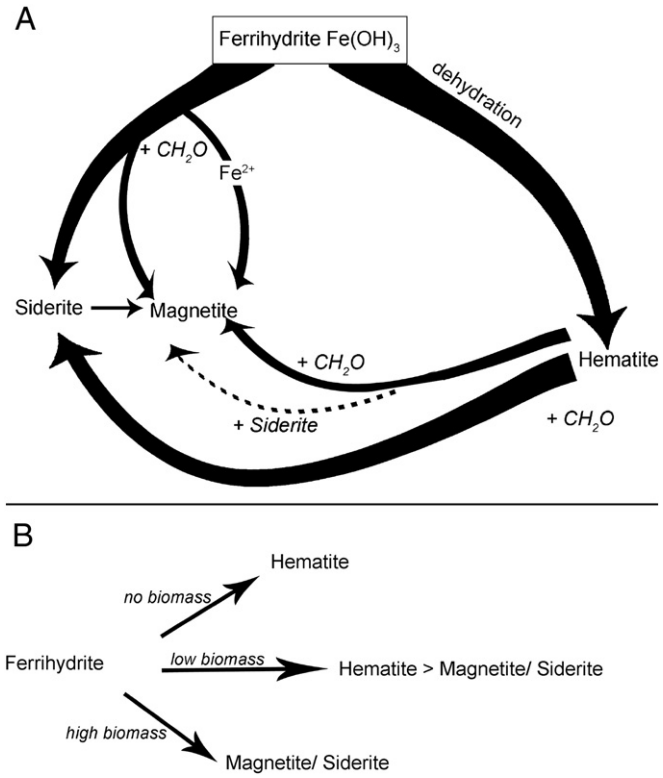

Fig. 4. (A) Mineral transformation pathways in capsule experiments. Ferrihydrite dehydrates to form hematite. With addition of biomass (CH_2O) in the form of glucose, siderite can form from ferrihydrite or from hematite. Hematite or ferrihydrite and glucose can form siderite magnetite. A theoretical formation of magnetite by hematite and siderite is represented by the dashed line. (B) The influence of biomass on the mineral product.

Three main avenues of investigation may offer further insight. First, a BIF sedimentary basin would likely harbor dissimilatory Fe(III)-reducing bacteria (Johnson et al., 2008). These microorganisms are known to produce siderite and magnetite (Lovley et al., 1993) and their biomass would offer an electron source for a variety of microorganisms. Experiments in which microbially-cycled minerals are treated to relevant temperature and pressure conditions will reveal more about the impact of these processes. Second, refractory forms of carbon, like kerogen or graphite instead of a glucose proxy may be used to better understand interaction of labile and refractory carbon over time. Third, as estimates for the dissolved silica concentration of the Archean ocean range upwards to 2.2 mM, the influence of shifting Si:Fe ratios needs to be tested.

Experimental diagenesis as carried out in this study can complement previous work to estimate the extent of the biological footprint on the early Earth (e.g., Mojzsis et al., 1996; Van Zuilen et al., 2002; Heimann et al., 2010; Steinhoefel et al., 2010). Recent discussion of the faint young sun paradox has brought fundamental questions of BIF diagenesis and mineral transformations to the fore (Rosing et al., 2010, 2011). Undoubtedly, an exchange between the atmosphere and oceans took place in the Archean, yet all pathways from the atmosphere to the seafloor are not yet constrained. It is known that Fe(III)-reducing bacteria can produce siderite and magnetite and thus regulate porewater conditions. Herein, it is demonstrated that siderite as well as hematite and magnetite formed from mixtures of Fe(III) mineral and organic matter in ratios that are typically found in biogenic minerals, however, without gaseous exchange. Atmospheric conditions, such as CH_4 and CO_2 concentrations are decoupled from these systems. This demonstrates a constraint on reading the rock record as a proxy of ancient atmospheres. Our data therefore suggests that atmospheric concentrations of methane and CO_2 during the time of BIF mineral deposition cannot be determined from BIF mineralogical data alone.

Acknowledgments

We thank Nicolas Beukes and Gert Van der Linde for the samples and discussion, Bernd Steinhilber, Daniel Russ and Indra Gill-Kopp for sample preparation and Melanie Keuper for Raman-spectroscopy. NP thanks Minik Rosing, Christian Bjerrum and Emily Pope for helpful discussion. This work was supported by the Wilhelm-Schuler Stiftung, the International PhD program GeoEnviron (German Academic Exchange Service (DAAD)), and research grant (PO 1624/1-1, 2-1) from the German Research Foundation (DFG) to NP, research grants (KA 1736/4-1 and 12-1) from the German Research Foundation (DFG) to AK, the Nachwuchsprogramm Universität Tübingen (for AK and BB), the Promotionsverbund "Einblicke in die Bakterien-Material-Wechselwirkungen" to IK, the National Science Foundation (Grant No. 1064391) to ES, and the Natural Sciences and Engineering Research Council of Canada to KK.

Appendix A. Supplementary data

Supplementary data to this article can be found online at http://dx.doi.org/10.1016/j.chemgeo.2013.05.031.

References

Anbar, A.D., Duan, Y., Lyons, T.W., Arnold, G.L., Kendall, B., Creaser, R.A., Kaufman, A.J., Gordon, G.W., Scott, C., Garvin, J., Buick, R., 2007. A whiff of oxygen before the Great Oxidation Event? Science 317, 1903–1906.
Bekker, A., Slack, J.F., Planavsky, N., Krapež, B., Hofmann, A., Konhauser, K.O., Rouxel, O.J., 2010. Iron formation: a sedimentary product of the complex interplay among mantle, tectonic, and biospheric processes. Economic Geology 105, 467–508.
Burt, D.M., 1972. The System Fe–Si–C–O–H: A Model for Metamorphosed Iron Formations. Carnegie Institute Washington Yearbook 1971–1972 435–443.
Cloud, P., 1968. Atmospheric and hydrospheric evolution on the primitive earth. Science 160, 729–736.
Cornell, R.M., Schwertmann, U., 2003. The Iron Oxides: Structures, Properties, Reactions, Occurrences and Uses. Wiley-VCH Verlag, Weinheim.
Craddock, P.R., Dauphas, N., 2011. Iron and carbon isotope evidence for microbial iron respiration throughout the Archean. Earth and Planetary Science Letters 303, 121–132.
Dimroth, E., Chauvel, J.J., 1973. Petrography of the Sokoman Iron Formation in part of the central Labrador Trough, Quebec, Canada. Geological Society of America Bulletin 84, 111–134.
Eglinton, T.I., 2012. A rusty carbon sink. Nature 483, 165–166.
French, B.M., 1971. Stability of siderite (FeCO3) in the system of Fe–C–O. American Journal of Science 271, 37–78.
Frost, R.L., Weier, M.L., 2004. Thermal decomposition of humboldtine — a high resolution thermogravimetric and hot stage Raman spectroscopic study. Journal of Thermal Analysis and Calorimetry 75 (1), 277–291.
Frost, C.D., von Blanckenburg, F., Schoenberg, R., Frost, B.R., Swapp, S.M., 2007. Preservation of Fe isotope heterogeneities during diagenesis and metamorphism of banded iron formations. Contributions to Mineralogy and Petrology 153, 211–235.
Hamade, T., Konhauser, K.O., Raiswell, R., Goldsmith, S., Morris, R.C., 2003. Using Ge/Si ratios to decouple iron and silica fluxes in Precambrian banded iron formations Geology 31, 35–38.
Han, T.-M., 1966. Textural relations of hematite and magnetite in some Precambrian metamorphosed oxide iron-formations. Economic Geology 61, 1306–1310.
Han, T.-M., 1978. Microstructures of magnetite as guides to its origin in some Precambrian iron-formations. Fortschritte der Mineralogie 56, 105–142.
Hansel, C.M., Benner, S.G., Neiss, J., Dohnalkova, A., Kukkadapu, R.K., Fendorf, S., 2003. Secondary mineralization pathways induced by dissimilatory iron reduction of ferrihydrite under advective flow. Geochimica et Cosmochimica Acta 67, 2977–2992.
Heaney, P.J., Veblen, D.R., 1991. An examination of spherulitic dubiomicrofossils in Precambrian banded iron formations using the transmission electron microscope. Precambrian Research 49, 355–372.
Heimann, A., Johnson, C.M., Beard, B.L., Valley, J.W., Roden, E.E., Spicuzza, M.J., Beukes, N.J., 2010. Fe, C, and O isotope compositions of banded iron formation carbonates demonstrate a major role for dissimilatory iron reduction in 2.5 Ga marine environments. Earth and Planetary Science Letters 294, 8–18.
Holland, H.D., 1973. The oceans: a possible source of iron in iron-formations. Economic Geologist 68, 1169–1172.
Holm, N.G., 1989. The $^{13}C/^{12}C$ ratios of siderite and organic matter of a modern metalliferous hydrothermal sediment and their implications for banded iron formations. Chemical Geology 77, 41–45.
Johnson, C., Beard, B.L., Klein, C., Beukes, N.J., Roden, E.E., 2008. Iron isotopes constrain biologic and abiologic processes in banded iron formation genesis. Geochimica et Cosmochimica Acta 72, 151–169.
Jones, A.M., Collins, R.N., Rose, J., Waite, T.D., 2009. The effect of silica and natural organic matter on the Fe(II)-catalysed transformation and reactivity of Fe(III) minerals. Geochimica et Cosmochimica Acta 73, 4409–4422.

Kappler, A., Newman, D.K., 2004. Formation of Fe (III) minerals by Fe(II) oxidizing photoautotrophic bacteria. Geochimica et Cosmochimica Acta 68 (6), 1217–1226.
Kappler, A., Pasquero, C., Konhauser, K.O., Newman, D.K., 2005. Deposition of banded iron formations by anoxygenic phototrophic Fe(II)-oxidizing bacteria. Geology 33 (11), 865–868.
Klein, C., 2005. Some Precambrian banded iron formations (BIFs) from around the world. Their age, geologic setting, mineralogy, metamorphism, geochemistry, and origin. American Mineralogist 90, 1473–1499.
Koehler, I., Papineau, D., Konhauser, K.O., Kappler, A., 2013. Biological carbon precursor to diagenetic siderite spherulites in banded iron formations. Nature Communications 4, 1741.
Konhauser, K., Hamade, T., Raiswell, R., Morris, R.C., Ferris, F.G., Southam, G., Canfield, D.E., 2002. Could bacteria have formed the Precambrian banded iron formations? Geology 30, 1079–1082.
Konhauser, K., Newman, D.K., Kappler, A., 2005. The potential significance of microbial Fe(III) reduction during deposition of Precambrian banded iron formations. Geobiology 3, 167–177.
Konhauser, K.O., Amskold, L., Lalonde, S.V., Posth, N.R., Kappler, A., Anbar, A., 2007a. Decoupling photochemical Fe(II) oxidation from shallow-water BIF deposition. Earth and Planetary Science Letters 258, 87–100.
Konhauser, K.O., Lalonde, S., Amskold, L., Holland, H.D., 2007b. Was there really an Archean phosphate crisis? Science 315, 1234.
Krapež, B., Barley, M.E., Pickard, A.L., 2003. Hydrothermal and resedimented origins of the precursor sediments to banded iron formation: sedimentological evidence from the Early Paleoproterozoic Brockman Supersequence of Western Australia. Sedimentology 50, 979–1011.
Lalonde, K., Mucci, A., Ouellet, A., Gelinas, Y., 2012. Preservation of organic matter in sediments promoted by iron. Nature 483, 198–200.
Li, Y.L., Konhauser, K.O., Cole, D.R., Phelps, T.J., 2011. Mineral ecophysiological evidence for microbial activity in banded iron formation. Geology 39, 707–710.
Li, Y.L., Konhauser, K.O., Kappler, A., Hao, X.L., 2013. Experimental low-grade alteration of biogenic magnetite indicates microbial involvement in generation of banded iron formations. Earth and Planetary Science Letters 361, 229–237.
Lovley, D.R., Giovannoni, S.J., White, D.C., Champine, J.E., Phillips, E.J.P., Gorby, Y.A., Goodwin, S., 1993. Geobacter-metallireducens gen-nov, a microorganism capable of coupling the complete oxidation of organic-compounds to the reduction or iron and other metals. Archives of Microbiology 159, 336–344.
Maliva, R.G., Knoll, A.H., Simonson, B.M., 2005. Secular change in the Precambrian silica circle: insights from chert petrology. Geological Society of America Bulletin 117, 835–845.
Marocchi, M., Bureau, H., Fiquet, G., Guyot, F., 2011. In-situ monitoring of the formation of carbon compounds during the dissolution of iron(II) carbonate (siderite). Chemical Geology 290, 145–155.
McCollom, T.M., 2003. Formation of meteorite hydrocarbons from thermal decomposition of siderite ($FeCO_3$). Geochimica et Cosmochimica Acta 67, 311–317.
Miyano, T., 1987. Diagenetic to low-grade metamorphic conditions of Precambrian iron-formations. In: Appel, P.W.U., LaBerge, G.L. (Eds.), Precambrian Iron Formations. Theophrastus Publications, Athens, pp. 155–186.
Miyano, T., Klein, C., 1984. Evaluation of the stability relations of amphibole asbestos in metamorphosed iron formations. Journal of Mining and Geology 33, 213–222.
Mojzsis, S.J., Arrhenius, G., McKeegan, K.D., Harrison, T.M., Nutman, A.P., Friend, C.R.L., 1996. Evidence for life on earth before 3,800 million years ago. Nature 384, 55–59.
Morris, R.C., 1993. Genetic modelling for banded iron-formation of the Hamersley Group, Pilbara Craton, Western Australia. Precambrian Research 60, 243–286.
Neumann, U., Mücke, A., 1994. The importance of paragenetic sequences in manganese quartzites and banded iron-formations. Abhandlungen European Journal of Mineralogy 6, 340.
Ohmoto, H., 2003. Nonredox transformations of magnetite–hematite in hydrothermal systems. Economic Geology and the Bulletin of the Society of Economic Geologists 98, 157–161.
Pecoits, E., Posth, N.R., Konhauser, K.O., Kappler, A., 2009. Petrography and trace element geochemistry of Dales Gorge Banded Iron Formation: paragenetic sequence, source and implications for the palaeo-ocean chemistry. Precambrian Research 172, 163–187.
Perry, E.C., Tan, F.C., Morey, G.B., 1973. Geology and stable isotope geochemistry of the Biwabik Iron Formation, northern Minnesota. Economic Geology 68, 1110–1125.
Planavsky, N., Rouxel, O., Bekker, A., Shapiro, R., Fralick, P., Knudsen, A., 2009. Iron-oxidizing microbial ecosystems thrived in late Paleoproterozoic redox-stratified oceans. Earth and Planetary Science Letters 286 (1–2), 230–242.
Posth, N.R., Hegler, F., Konhauser, K.O., Kappler, A., 2008. Alternating Si and Fe deposition caused by temperature fluctuations in Precambrian oceans. Nature Geoscience 1 (10), 703–708.
Posth, N.R., Huelin, S., Konhauser, K.O., Kappler, A., 2010. Size, density and composition of cell-mineral aggregates formed during anoxygenic phototrophic Fe(II) oxidation: impact on modern and ancient environments. Geochimica et Cosmochimica Acta 74, 3476–3493.
Posth, N.R., Konhauser, K.O., Kappler, A., 2011. Banded iron formations. In: Thiel, V., Reitner, J. (Eds.), Encyclopedia of Geobiology. Springer Verlag.
Posth, N.R., Konhauser, K.O., Kappler, A., 2013. Microbiological processes in BIF deposition. Sedimentology http://dx.doi.org/10.1111/sed.12051 (in press).
Robbins, E.I., Iberall, A.S., 1991. Mineral remains of early life on Earth? On Mars? Geomicrobiology Journal 9, 51–66.
Rosing, M.T., Bird, D.K., Sleep, N.H., Bjerrum, C.J., 2010. No climate paradox under the faint early sun. Nature 464, 744–749.
Rosing, M.T., Bird, D.K., Sleep, N.H., Bjerrum, C.J., 2011. Rosing, Bird, Sleep & Bjerrum reply. Nature 474, E4–E5.
Schwertmann, U., 1966. Inhibitory effect of soil organic matter on the crystallization of amorphous hydroxide. Nature 212, 645–646.
Sharma, P., Ofner, J., Kappler, A., 2010. Formation of binary and ternary colloids and dissolved complexes of organic matter, Fe and As. Environmental Science and Technology 44, 4479–4485.
Steinhoefel, G., von Blanckenburg, F., Horn, I., Konhauser, K.O., Beukes, N.J., Gutzmer, J., 2010. Deciphering formation processes of banded iron formations from the Transvaal and the Hamersley successions by combined Si and Fe isotope analysis using UV femtosecond laser ablation. Geochimica et Cosmochimica Acta 74, 2677–2696.
Summons, R.E., Jahnke, L.L., Logan, G.A., Hope, J.M., 1999. 2-Methylhopanoids as biomarkers for cyanobacterial oxygenic photosynthesis. Nature 398, 554–557.
Thamdrup, B., 2000. Bacterial manganese and iron reduction in aquatic sediments. Advances in Microbial Ecology, vol. 16. Kluwer Academic/Plenum Publ., New York 41–84.
Van Zuilen, M.A., Lepland, A., Arrhenius, G., 2002. Reassessing the evidence for the earliest traces of life. Nature 418, 627–630.
Walker, J.C.G., 1984. Suboxic diagenesis in banded iron formations. Nature 309, 340–342.
Widdel, F., Schnell, S., Heising, S., Ehrenreich, A., Assmus, B., Schink, B., 1993. Ferrous iron oxidation by anoxygenic phototrophic bacteria. Nature 362, 834–836.